Fitting a Radiation Mediated Shock Model of Gamma-Ray Bursts to the Band Model

Elliot Hansson
elliot.g.hansson@gmail.com

under the direction of
Filip Samuelsson
Department of Physics
KTH Royal Institute of Technology

Research Academy for Young Scientists
July 14, 2021

Abstract

Understanding the mechanisms of the prompt emission phase of gamma-ray bursts (GRBs) remains a difficult task. In this paper, a plausible radiation mediated shock model is examined and fitted against the Band model to determine how certain variations in the model parameters affect the parameters of the Band model. The scale parameter of the model was found to depend logarithmically on the α parameter of the Band model. It was also found that varying the $\tau\theta$ and Y_R parameter of the Komrad model affected the α as predicted, whereas the affects on α caused by varying the R parameter was inconclusive. The Band function data seem to follow distributions similar to that of Goldstein et al., but were ultimately not very similar in the range of the distributions. It was concluded that the data set was too small for a definite conclusion to be drawn regarding whether the model can resemble observational GRB data.

Acknowledgements

I would like to thank my mentor, Filip Samuelsson, for providing me with guidance and support throughout my research project. I would also like to thank my collaborator Arman Aspromonti for his valuable insights and conversations as well as his contributions with certain figures in my report. Furthermore, I would like to express my gratitude for Rays - for excellence, their organizers, and their collaborators Kjell & Märta Beijers Stiftelse and Kungl. Patriotiska Sällskapet.

Contents

1 Introduction

Gamma-ray bursts (GRBs) are the most energetic, powerful, and luminous events in the known universe, outshining its entire host galaxy during its most active phase. GRBs are the result of some of the most energetic explosions in the universe, resulting from supernovae or the merger of two binary neutron stars, shooting a burst of gamma-rays in the two directions of its source's spin. During the few seconds that a GRB typically lasts, it releases as much energy as our sun does during its entire ten billion year lifetime, approximately 10^{51} ergs. [1] Understanding the mechanisms that lead to these immensely powerful bursts is currently one of the biggest challenges within this field of research.

1.1 Background

In this section, central ideas to interpret the results are presented. If the reader is already familiar with the emission mechanisms of GRBs, please skip to section 1.1.2.

Gamma-ray bursts are typically divided into two phases, the prompt emission phase and the afterglow phase. The prompt emission phase is commonly measured by the time interval between which 5% and 95% of the total fluence (erg/cm^2) is detected, defined by the T_{90} parameter. The most notable challenge with understanding the prompt emission phase of GRBs is that the light curves produced are irregular and inconsistent. The afterglow phase, on the other hand, can last up to several years and shows a smooth and characteristic behavior. [2]

GRBs have been associated with supernovae, neutron star-neutron star mergers, and could potentially be associated with neutron star-black hole mergers as well. In particular, short GRBs are thought to originate from when two binary neutron stars merge. The mechanisms of how GRBs arise are uncertain, though many models attempt to predict the light curves observed from GRBs. These models also attempt to predict the efficacy of the burst. Half, or possible more than half of the explosion energy produced is converted into gamma rays. [1] The photon energy spectra produced when observing GRBs show

both a high energy part and a low energy part, and recent observations suggest that the two may have a separate physical origin [2].

The primary source of photons in GRBs is from braking radiation, which occurs when a charged particle, typically an electron, is deflected and decelerated by the electric field of another charged particle, which subsequently releases a photon to satisfy the law of conservation of energy. Similarly, magnetic fields can deflect and decelerate charged particles also producing photons, known as synchrotron radiation. [1]

Another concept relevant to the emission mechanisms of GRBs is Compton scattering. The high density of matter and photons present within the jet of a GRB inevitably leads to interactions between the photons and particles. A photon can transfer some of its energy to electrons, thereby increasing its wavelength, given that the photon is more energetic. Contrarily, if the electron is more energetic, the photon can gain energy from the electron, known as inverse Compton scattering. The large gain in energy that inverse Compton scattering causes on photons can have a significant impact on the observed photon energy spectra (hereby referred to as spectra). [3]

1.1.1 The Compactness Problem

When a photon with high enough enough energy ($E > 1.022MeV$) interacts with the electric field of an atomic nucleus, the photon undergoes pair production and produces an electron-positron pair ,$\gamma \rightarrow e^- + e^+$, in accordance with Einstein's equation, $E = mc^2$ [4]. This process would lead to the conclusion that the photons present within the jet should not escape due to the high density of particles now present in front of them, and this was coined The Compactness Problem. The fact that GRBs are observed, however, led to the conclusion that the outflow of GRBs must be traveling toward the Earth at highly relativistic speeds, causing Doppler blueshift making the photons appear significantly more energetic than they initially were at the outflow. [1]

1.1.2 Prompt Emission Models

The cause of the GRB emissions remains poorly understood, but several models attempt to explain the inconsistent light curves that are observed. The Fireball Model is one such candidate, for which it holds that the outflow is relativistic and that the photons can not escape due to the jet being optically thick. In the Fireball model, initial energy in the form of gravitational or rotational energy is converted into a high amount of radiation, which subsequently collides with the matter in the outflow, donating their energy to the particles, also known as Compton Scattering. The idea is that as the ejecta expands, it cools and the energy of the photons is converted into bulk kinetic energy, eventually releasing a burst of energy and matter. This burst is expected to have reached thermal equilibrium, meaning that the observed spectra should represent that of a black body. The spectra produced by GRBs, however, suggest that the kinetic energy must be reconverted into high-energy radiation in the outflow. [1]

The Photospheric Model is one candidate for describing the observed spectra. In the Photospheric Model, existing photons interact with electrons, positrons and baryons in the region of the outflow that is optically thick. As the outflow expands and cools, it will eventually become more likely for the photons to escape than to interact another time. This is conventionally defined for when the optical depth, τ is equal to 1. Mathematically, this produces a probability of the photon escaping to be $\approx 37\%$. The probability is given by $P = \mathrm{e}^{-\tau}$ [5]. The area for which this holds true is labeled the photosphere and inevitably results in the release of a GRB [1]. Important to note, however, is that the photosphere is defined statistically. Not all photons will escape at the photosphere specifically, and it would be more accurate to label the photosphere a volume rather than a radius. [1]

A Radiation Mediated Shock (RMS), is a process in which the gamma-ray burst is mediated by hot, non-thermal radiation. Firstly, photons influx the RMS zone from the upstream zone, likely originating from braking radiation and synchrotron radiation. The high amount of energy inevitably leads to a shock, releasing the radiation into the

downstream zone where it eventually passes the photosphere, and the GRB is released. [6]

1.1.3 The Band Model

The photon energy spectra of GRBs have historically been fitted to an empirical model called the Band Model in order to avoid biases toward a preferred physical emission model [2]. The Band Model can be represented by the Band function shown in equation (1)

$$N_{ph}(E) = A \begin{cases} (\frac{E}{100\,keV})^{\alpha}\ \exp\,(-\frac{E}{E_0}) & E < (\alpha-\beta)\,E_0 \\ \left[\frac{(\alpha-\beta)E_0}{100\,keV}\right]^{\alpha-\beta}\ \exp\,(\beta-\alpha)(\frac{E}{100\,keV})^{\beta} & E \geq (\alpha-\beta)\,E_0 \end{cases} \tag{1}$$

where $N_{ph}(E)$ are the photon number spectra, α the lower energy spectral slope, β the high energy spectral slope, E_0, the break energy, (referred to as xp in this study), and A, a normalization factor [2]. Although the model can not in itself provide any insight as to the physical origin of GRB emissions, comparing the Band model fits to the predictions of theoretical models can provide such insight [2].

1.1.4 Fermi Telescope Observational Window

The Fermi Gamma-ray Space Telescope, a satellite-based apparatus used for monitoring gamma-ray bursts, has two instruments, both the Large Area Telescope (LAT) and the Gamma-Ray Burst Monitor (GBM). The two instruments can only detect certain ranges of photon energies. The LAT can detect photons with an energy in the range of 30 MeV to more than 300 GeV, whereas the GBM has a range within 8 keV and overlaps with the lower energy parts of the LAT [7]. These boundaries are not definite, but rather the efficacy of detecting photons at the lower and upper energy boundaries decreases.

As can be seen in Figure 1 where the dashed lines mark the observational window, determining the low energy spectral slope, α, becomes difficult as the spectra shift to lower energy levels. The decrease in detected photons at the lower- and upper bound of the

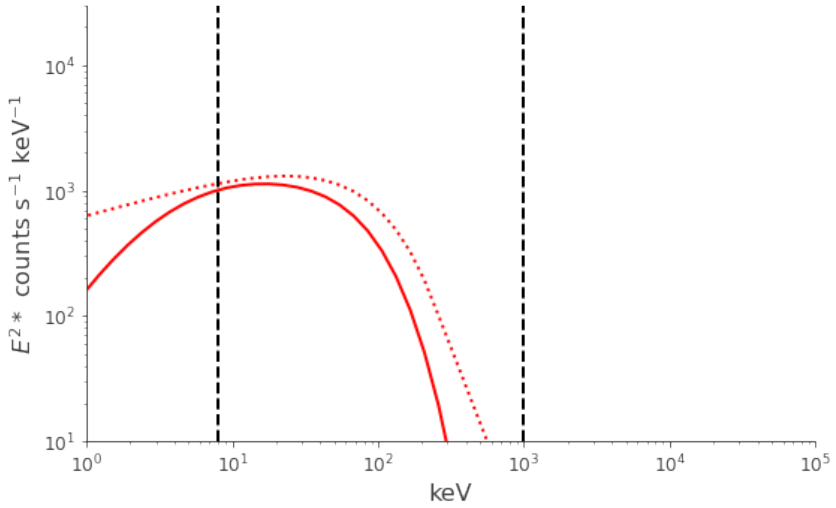

Figure 1: Synthetic spectrum in solid line and Band Function Fit in dotted line. The two vertical dashed lines mark the observational window of the GBM.

observational window also has to be accounted for.

1.2 Aim of Study

The aim of this study was to obtain a relationship between variations in the scale parameter of the Komrad model (see below for explanation of Komrad) and study its effects on the α parameter of the Band function. Based on any potential correlation between the two variables, the study aims to identify methods of predicting the slope of the low energy spectral slopes when the scale parameter of the Komrad model is enlarged. Ultimately, the study also aims to study which Komrad parameters most closely match the α values of observed GRB spectra.

2 Method

Recording gamma ray bursts is a difficult task. GRBs can originate from billions of light years away, meaning that only a few hundred or less photons reach the observing satellites. Cosmic background radiation, among other sources, can easily render the data of GRBs indistinguishable from noise. This challenge, along with the uncharacteristic nature of

the prompt emission phase of GRBs, has also led to a new method of analysis. Model spectra were first chosen, the parameters of the spectra were varied, and then fitted to a model of analysis, the Band Model, to determine the minimal difference between the model and data. [2]

2.1 Algorithm

To generate the synthetic spectra required in this study, the Komrad model was used. In the Komrad Model, a computer algorithm was used to generate radiation spectra based on a subphotospheric radiation mediated shock emission model.

Firstly, 125 synthetic spectra were created and subsequently imported to the Komrad-model. In generating the synthetic spectra, the parameters $\tau\theta$, R, and Y_R were varied randomly within a log-space. Since the initial 125 spectra were generated using response files from the Fermi Gamma-Ray Space Telescope, the synthetic spectra generated when varying each of the three parameters in the model generated a spectra similar to that of real GRBs.

Each synthetic spectra generated was then fitted to the Band function by determining the best fit values of the parameters of the Band function, α, β, and xp using regression of the model. By saving the data structure of the parameters being varied as well as the data structure of the corresponding Band parameter, the spectrum parameter could be plotted against the Band parameter to study the effects.

2.2 Parameters

The algorithm uses five essential parameters that were varied in the experiments. The $\tau\theta$ parameter effectively combines the temperature of the shock, θ_R and the optical depth, τ, that is, the probability of photon-particle interactions or Compton scattering. As such, $\tau\theta$ provides information regarding the downstream thermalisation and can be used to determine the energy of the photons released in the jet. The R parameter is a ratio

between the temperature of the RMS, θ_R and the temperature of the upstream photons θ_U. The Y_R parameter is a measure of the time that photons spend within the RMS, which essentially determines the amount of scatterings within the shock, and thus the energy of the photons. The optical depth, τ, is a measure of the amount of scatterings and how much the spectrum thermalizes before it reaches the photosphere.

The scale parameter is a measure of the shift of a spectrum with respect to the independent axis, the energy of the photons, with a photon count on the dependent axis, illustrated in Figure 2. Although scale is not directly linked to any processes within a GRB, it is related to the speed of the outflow. A faster outflow will result in more blueshift of the photons to higher energy levels, whereas a slower outflow will make the spectrum tend toward lower energy levels.

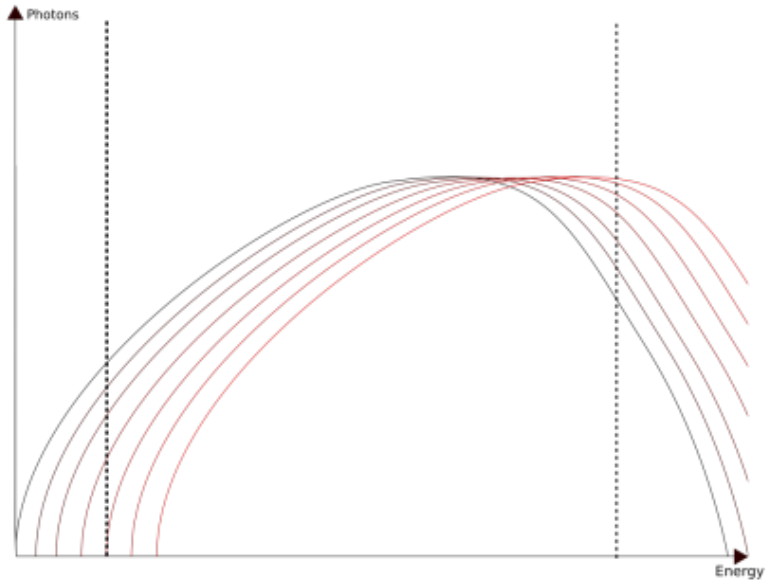

Figure 2: Arbitrary GRB spectrum illustrating the effects of varying the scale parameter, increasing from black to red with arbitrary units. The dashed lines mark the observational window.

The Signal-Noise Ratio, SNR, represents the ratio between the signal from the GRBs and the background radiation of space. The algorithm works by keeping the noise constant, and multiplying the signal by the SNR (See Figure 3). This parameter is important in order to study spectra produced by the model without the interference of noise.

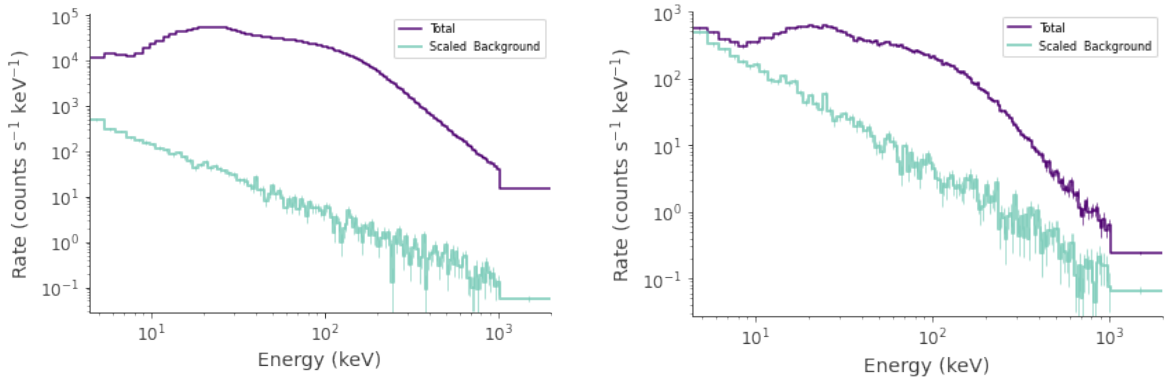

(a) SNR = 1000

(b) SNR = 10

Figure 3: Graph illustrating the effects of varying SNR. Both graphs have the same values of $\tau\theta$, R, and Y_R: 5, 200, and 1.5, respectively. The increased Signal-Noise Ratio on graph a clearly shows a higher peak of photon counts (note exponential scale).

2.3 Analysis of results

The computer algorithm allows for variation in the parameters $\tau\theta$, R, and Y_R as well as the Signal-Noise ratio (SNR), and scale (shift with respect to the independent axis). By varying the scale of the spectra generated, the effect on the α values of the Band function fit could be observed and subsequently plotted against the scale. Additionally, all five parameters were varied and the α values of the Band-function were recorded. A histogram was created with the recorded values of α to visualize the distribution and to compare it with observational GRB data.

3 Results

In Figures 4-6, the Komrad parameters were varied and the α parameter that each spectra was fitted against was subsequently plotted to study the correlation between variations in the Komrad model parameters and the Band function fit parameters. In Figure 7, a histogram was plotted with the corresponding value of each Band function parameter plotted against the number of spectra.

In Figure 4a, Band α shows a strong logarithmic-scale correlation as the scale in-

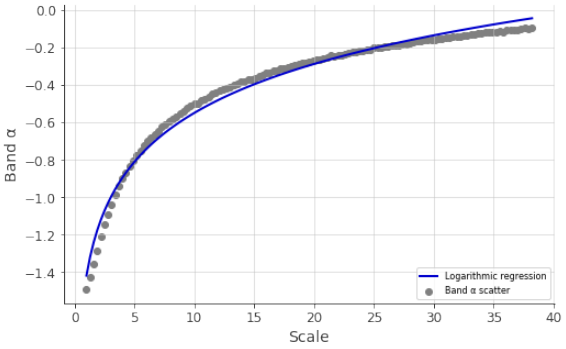

(a) SNR = 1000

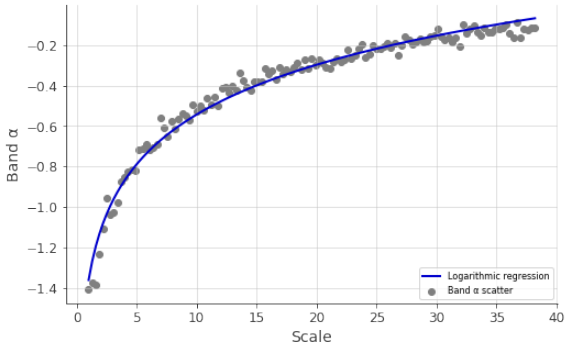

(b) SNR = 10

Figure 4: In both graphs, $\tau\theta$, R, and Y_R remain constant with values of 5, 200 and 1.5 respectively. The scale is increased linearly within the range 1 to 38.2, increasing with 0.3 for each spectra. In Figure 5a, the SNR is equal to 1000 whereas in Figure 5b, the SNR is equal to 10. The logarithmic regression line in graph (a) and graph (b) is approximately $0.377\log(x) - 1.42$ and $0.355\log(x) - 1.36$, respectively.

creases. In Figure 4b, the data is more scattered but the logarithmic-scale correlation remains mildly strong. In both graphs of Figure 4, Band α appears to approach a value within the range $\alpha \in (-0.25, 0)$ as the scale increases.

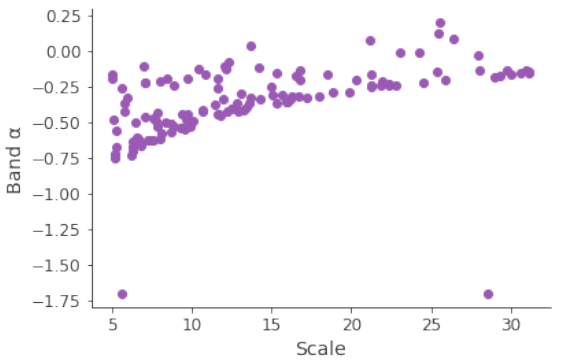

(a) SNR = 1000

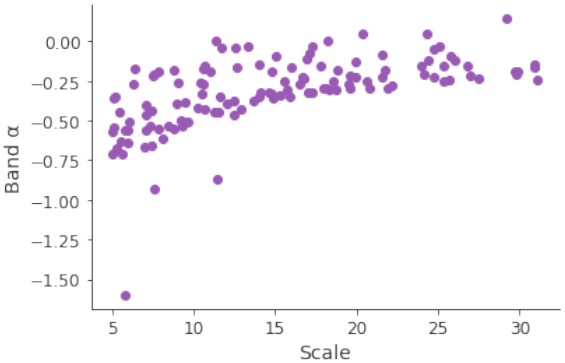

(b) SNR = 10

Figure 5: In both graphs, the parameters $\tau\Theta$, R, Y_R, and scale vary randomly in log-space within the ranges $(3, 30)$, $(30, 300)$, $(0.5, 3)$, and $(4, 25)$, respectively. In graph (a), the SNR is equal to 1000 whereas in graph (b), the SNR is equal to 10, demonstrating the robustness to noise.

In the graphs of Figure 5, all parameters except for the SNR were randomly varied within the log-space specified in the caption. Band α still showed a logarithmic-scale correlation when the scale increased.

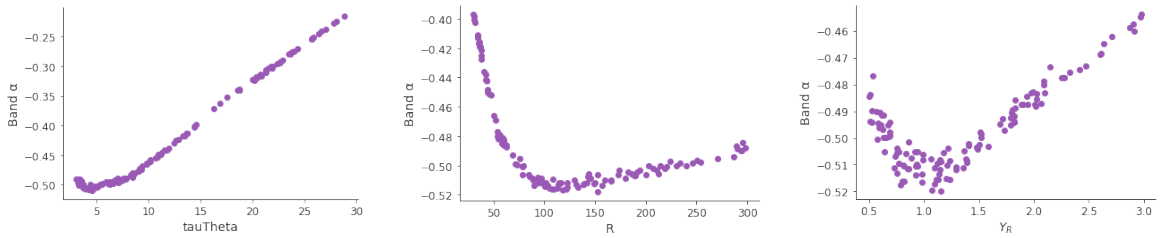

(a) $\tau\theta \in (3, 30)$ (b) $R \in (30, 300)$ (c) $Y_R \in (0.5, 3)$

Figure 6: Graphs (a), (b), and (c) show the relationship between $\tau\theta$, R, Y_R, respectively, and Band α.

In Figure 6, the three graphs show the relationship between $\tau\theta$, R, and Y_R as they vary randomly in log-space within the captioned ranges. Figure 6a shows a seemingly linear relationship after an initial polynomial relationship, while in Figure 6b, alpha appears to initially decrease at a decelerating rate for $R \in (30, 100)$ followed by a linear increase for $R \in (100, 300)$. Finally, Figure 6c shows a scattered decline in Band α for $Y_R \in (0.5, 1)$ and then a linear increase for $Y_R \in (1, 3)$.

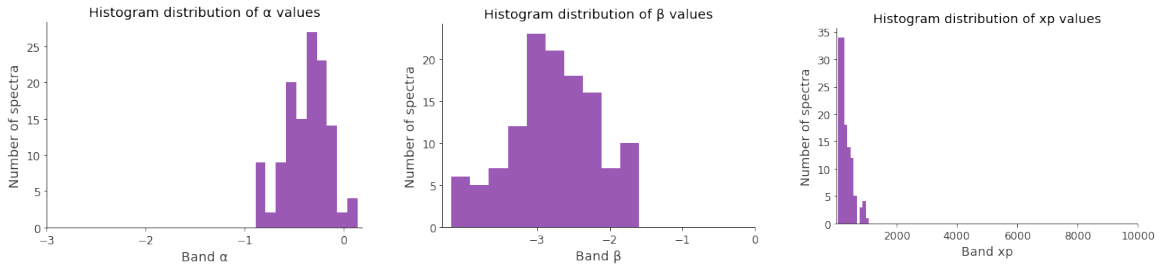

(a) Distribution of Band α among 125 spectra (b) Distribution of Band β among 125 spectra (c) Distribution of Band xp among 125 spectra

Figure 7: The graphs show a histogram distribution of the fitted Band function parameters α, β, and xp among 125 spectra with random values of the parameters $\tau\theta$, R, Y_R, SNR and scale with ranges of (3, 30), (30, 300), (0.5, 3), (5, 50) and (4, 25), respectively.

In Figure 7, three histograms were plotted to illustrate the distribution of the Band function fits α, β, and xp with the number of fits on the dependent axis, and the fitted value on the independent axis.

4 Discussion

The logarithmic correlation between the α parameter and scale parameter can be graphically illustrated with the Band function fit. The α variable, essentially determining the slope of the lower spectral energy part of the Band function, increases as the spectrum moves toward higher energy levels and then continues indefinitely at the same slope, presumably with a constant value of α. This also follows from Figure 4a and 4b as the data points appear to approach an α value within the range (-0.25, 0). The logarithmic fit would suggest an indefinite increase in α. However, it appears that the logarithmic fit crosses below the scatter plot when the scale is within the range (5, 25), and it also goes above the scatter when scale reaches above 25. This suggests that the value of α does not follow the logarithmic regression line afterward and is most accurate within the range (4, 25).

It can be inferred that scale values below the value of 4 or above the value of 25 can produce skewed results as the α increase is significantly larger in the range (0, 4) and significantly lower as scale goes above 25, suggesting that varying the scale parameter within the range (4, 25) would produce the most accurate results when varying other parameters of the Komrad model.

To determine whether scale showed a correlation with α when the other parameters were varied, the experiments plotted in Figure 5 were conducted. An increase in the scale parameter still showed a correlation with an increase in the α parameter. The change in α was obviously shorter, due to the shorter range in the scale parameter. These results were obtained regardless of the signal to noise ratio. This correlation can be explained by the fact that increasing the scale will display more of the graph within the observational window of the telescope, which the Komrad model accounts for. The Band function fit for the α parameter would thus increase as the slope within the observational window increases until it finally becomes constant as the lower energy spectral slope continues indefinitely, this is illustrated in Figure 2

In Figure 6, the three parameters $\tau\theta$, R, and Y_R were varied to study its effect on the Band α parameter. $\tau\theta$ showed a positive and seemingly linear relationship with α. Since $\tau\theta$ essentially is a measure of the Comptonization and thus thermalisation in a jet, it can be inferred that an increase in the $\tau\theta$ parameter would result in photons tending toward the middle of the spectrum to resemble more of a black body. The increase in the photons would increase the slope up to the peak energy, thus increasing the value of α.

In varying the R parameter, values within the range (30, 100) appeared to be decreasing at a decelerating rate, that is, with a positive second-derivative with respect to R, followed by a linear increase in the range (100, 300). Higher values of R should increase the value of α proportionally, but the decline of α within the range (30, 100) is inconclusive.

Finally, varying the Y_R parameter showed a more scattered plot with a decrease in the value of α in the range (0.5, 1.2) and then an increase in the range (1.2, 3). Similarly to the variations in $\tau\theta$, higher values of Y_R will increase Comptonization and thermalization, and photons will tend to the middle of the spectrum energy, thereby increasing the slope and thus the value of α.

Lastly, three histograms were created where the values of α, β, and xp were plotted for each spectra. The distribution of all parameters were in fact quite different from that of observational GRB data. Goldstein et al. [8] showed a distribution of α values with a similar shape of which was obtained in Figure 7a, although centered around $\alpha \approx -1$ with few α values nearing -2 and 0. The distribution of β and xp, however, did not show a similar shape nor distribution to what was obtained by Goldstein et al., but this can be explained by the lack thereof accuracy when it comes to higher energy levels. However, it must be considered that Goldstein et al. processed considerably more data. Goldstein et al. plotted Band function fits from 3800 GRB spectra, whereas Figure 5 only considered 125 synthetic GRB spectra.

4.1 Further studies

Since studies with first-principle radiation-hydrodynamics simulations are computationally expensive to run, RMS models such as the Komrad model must be considered in finding an accurate emission model for GRBs. In order to further test the accuracy of the model, it is important to determine whether the model is capable of producing similar distributions of the Band function parameters to that of real GRBs, such as the distributions provided by Goldstein et al. Additionally, the model must be able to predict the efficacy of the burst. The model parameters $\tau\theta$, R, and Y_R all denote physical processes within the RMS, meaning that the model must be able to account for all physical processes that may or may not contribute to the amount of photons and their energies.

Mathematically approximating these parameters from real GRBs may be done given enough information, such as spin and mass of a supernova or two binary stars. They are, however, difficult to detect in the first place and as such, any additional information about the binary stars would be difficult to acquire.

4.2 Conclusion

Ultimately, a logarithmic relationship between the scale parameter of the Komrad-model and the Band α parameter could be established and subsequently explained by the fact that the first power law of the Band function fit would move to higher energy levels as the scale increases, thereby increasing the lower energy spectral slope variable of the Band function α as more of it is present within the observational window. It is also suggested that the proportional increase of α as $\tau\theta$ increased relates to the amount of Comptonization in the jet, subsequently moving the first power law to lower energy levels, the same was observed with Y_R in which an increase in the parameter would increase Comptonization. For the R parameter, however, the initial decrease in the value of α remained inconclusive.

Analysis of the obtained Band function fits with observational GRB data concluded

that the parameters used in the Komrad model, when plotted with a histogram, did not resemble that of observational GRB data from Goldstein et al. This could, however, be explained by the difference in the amount of spectra and further studies generating more synthetic spectra are required to see if the Komrad model can produce similar distributions.

References

[1] Samuelsson F. Multi-messenger emission from gamma-ray bursts. KTH Royal Institute of Technology; 2020.

[2] Pe'Er A. Physics of gamma-ray bursts prompt emission. Advances in Astronomy. 2015;2015.

[3] Iyyani S. Photospheric emission in gamma ray bursts: Analysis and interpretation of observations made by the Fermi gamma ray space telescope. Department of Physics, Stockholm University; 2015.

[4] Einstein A. Does the inertia of a body depend upon its energy-content. Ann Phys. 1905;18:639–641.

[5] Kitchin CR. Stars, nebulae and the interstellar medium: observational physics and astrophysics. CRC Press; 1987.

[6] Levinson A, Nakar E. Physics of radiation mediated shocks and its applications to GRBs, supernovae, and neutron star mergers. Physics Reports. 2020;866:1–46. Physics of radiation mediated shocks and its applications to GRBs, supernovae, and neutron star mergers. Available from: `https://www.sciencedirect.com/science/article/pii/S0370157320301265`.

[7] Garner R. Fermi Spacecraft and Instruments. NASA; 2017. Available from: `https://www.nasa.gov/content/goddard/fermi-spacecraft-and-instruments`.

[8] Goldstein A, Burgess JM, Preece RD, Briggs MS, Guiriec S, van der Horst AJ, et al. The fermi GBM gamma-ray burst spectral catalog: the first two years. The Astrophysical Journal Supplement Series. 2012;199(1):19.

A Appendix